Characteristics of Dielectric Behavior and AC Electrical Conductivity of Bulk Antimony Sulfide (Sb₂S₃)

H. E. A. El-Sayed, H. A. M. Ali[*], G. F. Salem, M. A. Mahmoud

Physics Department, Faculty of Education, Ain Shams University, Cairo, Egypt

The structural features and morphology of investigated Sb_2S_3 powder were analyzed using X-ray diffraction and scanning electron microscope techniques. The dependence of dielectric properties and ac conductivity of bulk Sb_2S_3 as pellet on both of frequency (10^2–10^6 Hz) and temperature (303-393 K) were studied. The dielectric constant (121.2-45.8) and dielectric loss (53.3-0.89) displayed noticeable dependence on frequency and in the investigated range of temperature 303-393 K. The frequency dependence of ac conductivity $\sigma_{ac}(\omega)$ follows up the power relation; $\sigma_{ac}(\omega) = G\omega^s$. The frequency exponent s, diminished with the rise in temperature, implying that the correlated barrier hopping (CBH) is the predominant conduction mechanism. The ac conductivity exhibited a thermally activated nature. The localized states $N(E_F)$ values were recorded in the order of 10^{18} $eV^{-1}.cm^{-3}$ at specific temperatures for frequency of 800 Hz. Activation energy ΔE, calculated at different frequencies indicates a decrease from 117 meV to 89 meV with the increase in the frequency.

Introduction

The Antimony sulfide, Sb_2S_3, is one of V-VI semiconductor materials and it exists in nature as mineral stibnite [1,2]. Antimony sulfide is one of the most promising semiconductor functional materials because of its characteristic structure [3,4] with orthorhombic crystal structure [1]. It is an n-type semiconductor [5] and has a considerable attention for usage in the electronic applications as photoconductive detectors [6], photo-catalysis [7], photovoltaics [8], thermoelectric devices [9]. Petzelt and Grigas [10] measured Far infrared reflectivity of Sb_2S_3 single crystals in the spectral region 25-400 cm^{-1} and temperature region 100-400 K in polarized light. The results suggested that Sb_2S_3 was polar in the whole temperature region investigated.

The large anisotropy of the structure for Sb_2S_3 crystal showed effects on the physical properties. The static dielectric constant parallel to the chain axis is more than ten times larger compared to that prependicular to the same axis [11-13]. Due to its excellent photoconductivity, Sb_2S_3 garbs a wide attention for its potential applications in solar energy conversions [14,15] and as an absorber layer in solar cells [1,16,17]. Messina et al. [18] prepared Sb_2S_3 thin films for photovoltaic cell. Additionally, it showed particular optical properties; high refractive index [19], and high optical absorption coefficient ($\alpha > 10^4$ cm^{-1}) [20-22].

Ghosh and Varma [23] studied some optical properties of amorphous and crystalline Sb2S3 thin film. They observed that the amorphous Sb_2S_3 films had values for imaginary and real parts of the

dielectric constant much less than the polycrystalline films. The optical gap in amorphous material observed at 1.7 eV compared to the apparently direct band gap of 1.88 eV observed in crystalline materials. Also, it was found that the electrical resistivity of the Sb_2S_3 thin films decreased from 10^8 to 10^6 Ω.cm after plasma treatments.

The present work aims at studying the dependence of dielectric properties (ε_1 and ε_2) and ac conductivity (σ_{ac}) of bulk Sb_2S_3 on both frequency and temperature. The frequency range is (10^2–10^6 Hz) and temperature range is 303-393 K. The predominant mechanism for ac conduction is specified. The behavior for electric modulus ($M^/$ and $M^{//}$) of bulk Sb_2S_3 is also investigated.

Experimental technique

The powder of Sb_2S_3 was purchased from BALZERS. Elemental analysis was carried out using Quanta FEG- 250 SEM instrument for energy dispersion analysis spectrum. X-Ray diffraction, XRD, technique was utilized for analyzing the structural properties of the Figure (2) displays the XRD pattern of Sb_2S_3. It has various diffraction peaks with different intensities, illustrating that the Sb_2S_3 has a polycrystalline nature. The position of the peaks appeared in the diffractogram of the powder sample agreement with JCPD card No. (87-1135) [26]. The structural features are consistent with an orthorhombic system with lattice parameters a= 14.20Å, b=11.47 Å, c=7.47 Å and density of 3.709 g/cm^3. The major diffraction peak corresponds to the preferred orientation of (401). In other studies, preferred orientation plane is (130) as published in the literature [1,27,28]. Figure (3a) shows the image of the surface morphology of Sb_2S_3. The powder of Sb_2S_3 showed particles of irregular shape which distributed over the surface in agglomerates as shown through the higher-magnification SEM image (Fig. 3(b)).

investigated Sb_2S_3. XRD pattern was detected using X-ray diffractometer (Philips, model x`pert) with the characteristic CuK_α radiation.

A compressed pellet was obtained from grounded Sb_2S_3 powder. Scanning electron microscopy was performed using SEM microscope Quantum FEG 250. The compression was under a pressure of 2×10^8 N/m^2. The pellet thickness and radius were 1.05 mm and 5 mm, respectively. Two silver electrodes were made on both sides of the pellet by

using thermal evaporation method. High-vacuum coating unit, Edwards 306A- England was used for the deposition under pressure of 10^{-4} Pa with a deposition rate of 2.5 nm/s. The AC and dielectric measurements for the investigated sample were carried out using a programmable automatic RLC bridge, Hioki model 3532 Hitester, in the frequency ranges (10^2–10^6 Hz). The temperature was measured using a thermocouple over temperature range (303–393K). The values of capacitance, C, and loss tangent, tanδ measuring from LCR Bridge were used to calculate the dielectric constant and dialectic loss as : $\varepsilon_1 = Cd/\varepsilon_oA$ and $\varepsilon_2=\varepsilon_1$ tanδ, respectively, where d is the thickness, A is the cross section area of the pellet and ε_o is the permittivity of free space. Additionally, ac conductivity of the sample (σ_{ac}) was estimated from the relation: $\sigma_{ac}= \omega\varepsilon_o\varepsilon_2$ [24,25] where ω is the angular frequency.

RESULTS AND DISCUSSION

1. Structural properties of Sb_2S_3

Figure (1) shows the EDX spectrum recorded on the powder of Sb_2S_3, whose peaks are assigned to Sb and S. A small peak for oxygen was observed as faint impurity as formation of antimony oxides during the preparation of the product. The EDX analysis of the Sb_2S_3 shows that the atomic percentage of (Sb ≈32.75%) is smaller than that of (S≈ 49.03%), where the ratio of Sb/S to be 0.667, as expected.

2. Frequency and temperature dependencies of dielectric properties

The study of dielectric properties for materials is an important to give information about the conduction processes. The complex permittivity is explained according to the following equation [29]:

$$\varepsilon^*(\omega) = \varepsilon_1(\omega) - i\varepsilon_2(\omega) \qquad (1)$$

The frequency and temperature dependences of the dielectric constant $\varepsilon_1(\omega)$ and dielectric loss $\varepsilon_2(\omega)$ were studied for bulk Sb_2S_3 in the frequency ranges (10^2–10^6 Hz) and temperature range (303–393) K. Fig.4(a,b) illustrate the frequency dependence of the dielectric constant $\varepsilon_1(\omega)$ and dielectric loss $\varepsilon_2(\omega)$ at the different temperatures. As seen, in the investigated range of temperatures, the dielectric constant showed values in the range from 121.2 to 45.8 and dielectric loss showed

values in the range from 53.3 to 0.89. The higher values of ε_1 (115±5) and ε_2 (36±17) appeared at While they decreased and approaching a constant value at high frequencies as 46±1 for ε_1 and 1.32 ±0.4 for ε_2 in the investigated range of temperatures. The decrease of $\varepsilon_1(\omega)$ probably refer to the contribution of many components of polarization; ionic, electronic, interface and orientation polarizations [30-32]. At greater frequencies, the dipole unable to follow up the field, and the orientation polarization stopped. Thus, the value of $\varepsilon_1(\omega)$ may be assigned to the space charge or interfacial polarization as observed in studies reported by other authors[33,34]. On the other hand, the behavior of $\varepsilon_2(\omega)$ at low frequencies is due to the migration of ions in the material. After average increase in frequency, value depends on the contribution of ions jump, conduction loss of ions migration, and ions low frequencies and in the investigated range of temperatures.

polarization loss. At higher frequency, ion vibrations give the source of dielectric loss and ε_2 exhibited a lower value.

Figure 5(a,b) represents temperature dependence of $\varepsilon_1(\omega)$ and $\varepsilon_2(\omega)$ at the certain frequencies. Both $\varepsilon_1(\omega)$ and $\varepsilon_2(\omega)$ increase with increasing temperature at various frequencies. At low temperatures, dipoles in polar materials cannot orient themselves. As the temperature increases, the orientation of dipoles becomes easier where it gave an increase in the orientational polarization and ε_1. The raising in the value of $\varepsilon_2(\omega)$ with the raise in temperature can be explained according to Stevels [32,35], who divided the relaxation phenomena into three parts, conduction loss, dipole loss and vibrational loss.
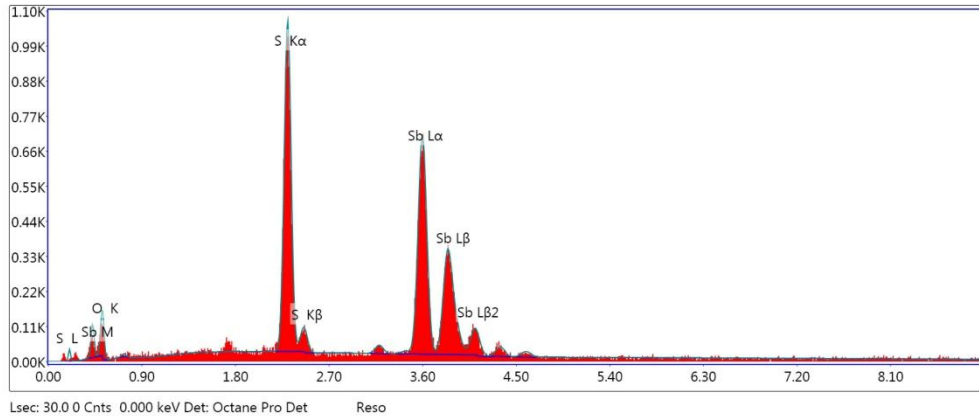
Fig. (1): EDX spectrum of Sb$_2$S$_3$

H. E. A. EL-SAYED et.al
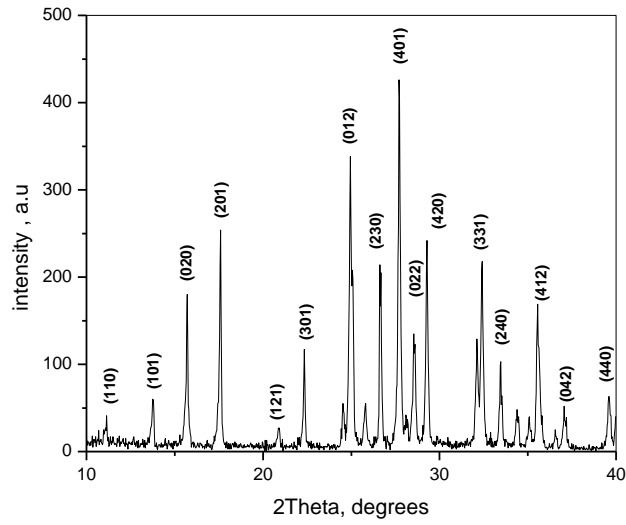
Fig. (2): XRD pattern of Sb$_2$S$_3$ in the powder form

(a)

(b)
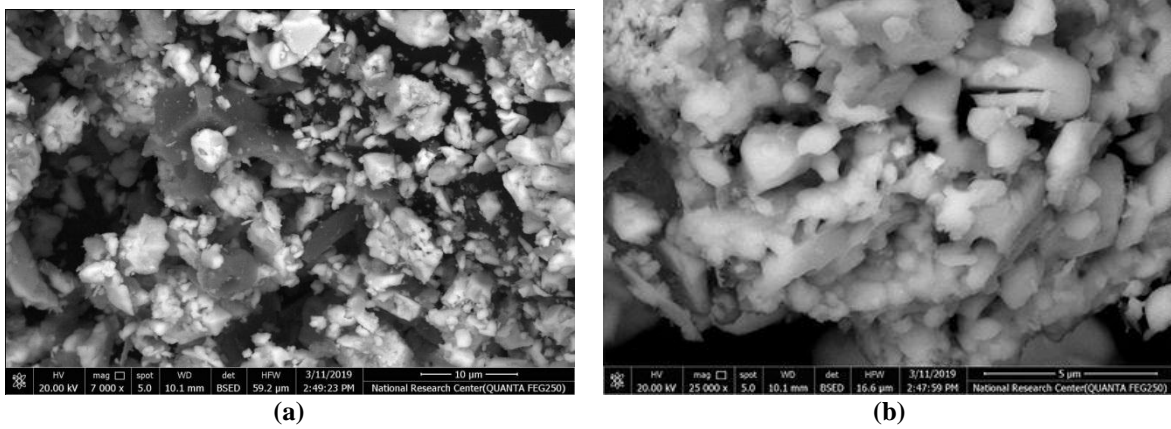
Fig. (3): SEM image of Sb$_2$S$_3$ at Magnification of (a) 7000x and (b) 25000x
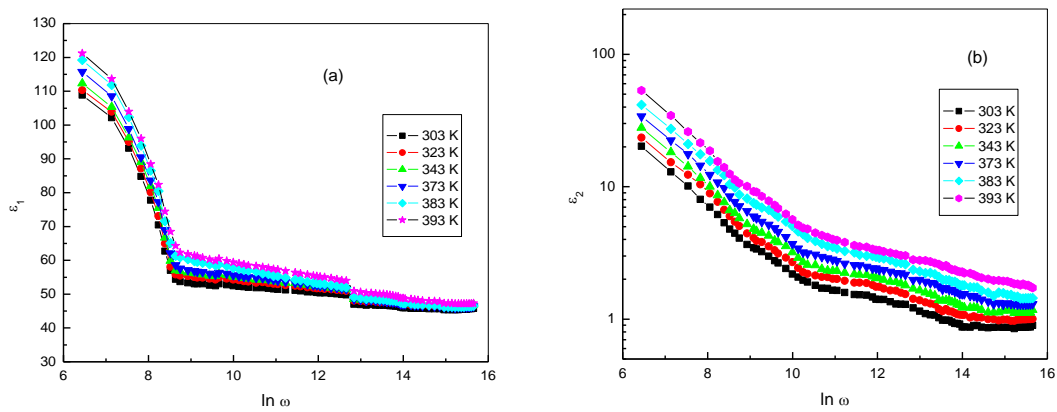
Fig. (4): Frequency dependence of (a) dielectric constant ε_1 (ω) and (b) dielectric loss ε_2 (ω) for Sb$_2$S$_3$ at different temperatures
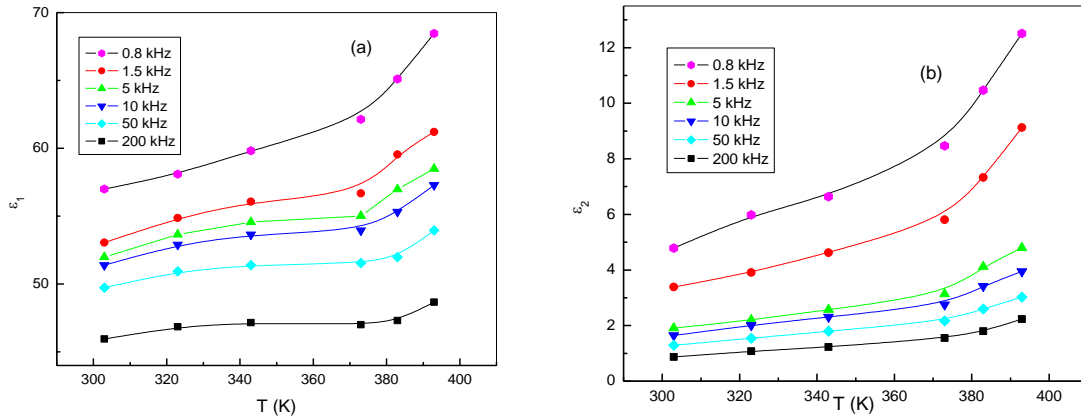
Fig. (5): Temperature dependence (a) dielectric constant ε_1 (ω) and (b)dielectric loss ε_2 (ω) for Sb$_2$S$_3$ at different frequencies

3. Electric modulus spectrum

The electrical relaxation of bulk Sb$_2$S$_3$ can be obtained from the studied electric modulus [36, 37]. The complex of electric modulus M* is given by

$$M^*(\omega) = M' + iM'' \qquad (2)$$

$$M' = \frac{\varepsilon_1}{\varepsilon_1^2 + \varepsilon_2^2} \qquad , \qquad M'' = \frac{\varepsilon_2}{\varepsilon_1^2 + \varepsilon_2^2}$$
(3)

Where, M$'$ and M$''$ are the real and imaginary parts of the dielectric modulus, respectively. The frequency dependence of the real and imaginary parts of the electric modulus M$'$ and M$''$ for bulk Sb$_2$S$_3$ at different temperatures are shown in Fig. 6, 7. It is noted that M$'$ has small values at low frequencies, 8.8×10^{-3} at 303 K and 6.9×10^{-3} at 393 K. It increases with the increase in frequency at different temperatures. The imaginary part of electric modulus M$''$ decreases at low frequencies, then it increases with raising the frequency which reaches a maximum value of 1.49×10^{-3} at 303 K and 2.66×10^{-3} at 393 K and after that it decreases with the further raise in frequency values.

4. AC conductivity

AC conductivity is an important factor which gives information about the transport phenomenon in materials, also it is a good method for determining the hopping dynamics of ions. The ac conductivity (σ_{ac}) showed dependence on the frequency of the applied field as a power relation [38]:

$$\sigma_{ac}(\omega) = G\omega^s \qquad (4)$$

Where, G is a pre-factor that depends on temperature and composition, and s is the frequency exponent that can take the value range from $0 < s \leq 1$ [39]. Figure (8) presents the variation of lnσ_{ac} for bulk Sb$_2$S$_3$ versus lnω at different temperatures. From this Figure, the ac conductivity for bulk Sb$_2$S$_3$ increases gradually with increasing the frequency. Then, it shows a great increase in its values. The frequency exponent (s) is calculated for the different temperatures (300-393 K). The dependence of s on temperature is seen in Fig.(9). It was observed that s values decreased with the increase in the temperature. This result for the frequency exponent is consistent with the observed for amorphous fast ion conducting Ag$_2$S–Sb$_2$S$_3$ materials [40] and Sb$_2$S$_3$ films [33] and Sb$_2$S$_3$ sprayed thin film [41]. The behavior of the frequency exponent is used to determine the type of the dominant mechanism for ac conduction [42]. Various models; quantum mechanical-tunneling model [43,44], small polaron tunneling model [44,45], correlated barrier hopping (CBH) model and large polaron tunneling model [46-48] have been suggested for ac conduction mechanisms in different materials. Depending on the obtained results for bulk Sb$_2$S$_3$

under investigation (Fig.9), the mechanism of ac conduction follows CBH model [47] as observed in Table (1) for other samples of Sb_2S_3. On Austin–Mott formula [49], based on CBH model, ac conductivity expressed as:

$$\sigma_{ac}(\omega) = \frac{\pi}{3}[(N(E_F)]^2 k_B T e^2 \alpha^{-5} \omega [ln(\nu_p/\omega)]^4 \quad (5)$$

Where, $N(E_F)$ is the density of localized states, k_B is the Boltzmann's constant, e is the electronic charge, α is the exponential decay parameter of localized states wave functions and ν_p is the frequency of the phonons. In CBH mechanism, σ_{ac} is interpreted according to hopping of electrons between pairs of localized states at the Fermi level $N(E_F)$. By assuming $\nu_p=10^{12}$ Hz and $\alpha^{-1}=10$ Å [50], $N(E_F)$ is calculated at different temperatures for frequency of 800 Hz and recorded in Table (2). The values of $N(E_F)$ for bulk Sb_2S_3 increases from 8.69×10^{18} to 12.09×10^{18} $eV^{-1}.cm^{-3}$ with the increase in the temperatures from 303 K to 393 K. These values of $N(E_F)$ are compared with other studies as seen in Table (2). Figure (10) shows the variation of ac conductivity for bulk Sb_2S_3 with 1000/T at different frequencies. It was observed that σ_{ac} increased linearly with the increase in the temperature. This behavior was attributed to the increase in the number of charges, which makes hopping increases [51]. This suggested that the ac conductivity for bulk Sb_2S_3 was a thermally activated process with an activation energy ΔE. The value of ΔE for ac conduction was calculated from the Arrhenius relation asfollows [52]:

$$\sigma_{ac} = \sigma_p (-\Delta E/k_B T) \quad (6)$$

Where, σ_p is a pre-exponential constant. The frequency dependence of ΔE for Sb_2S_3 is shown in Fig. (11). ΔE decreased with increasing frequency from 117 meV at 800 Hz to 89 meV at 200 kHz, which refers to the increase of the electronic jumps between the localized states as the applied frequency rises [53]. This emphasizes that the hopping conduction is the prevalent mechanism for ac conduction in Sb_2S_3. A similar trend was observed in Sb_2S_3 thin films [33].
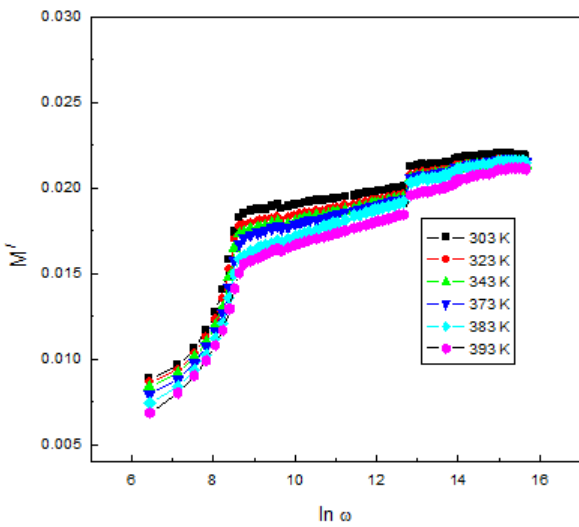
Fig. (6): Frequency dependence real part of dielectric modulus M' for Sb_2S_3 at different temperatures
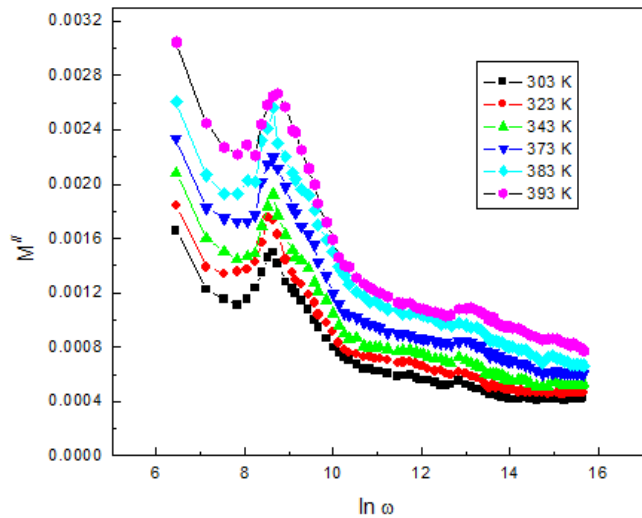
Fig. (7): Frequency dependence imaginary parts of dielectric modulus M'' for Sb_2S_3 at different temperatures
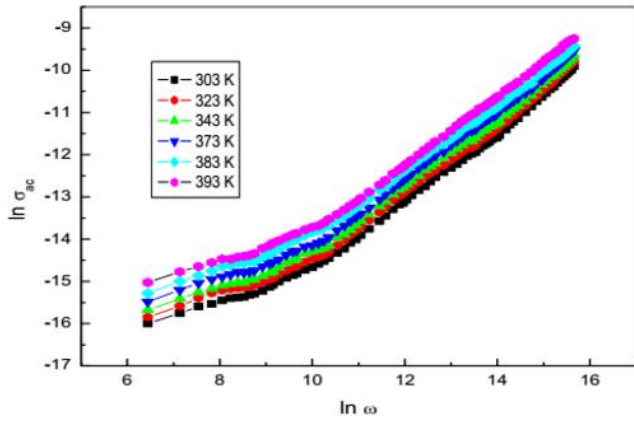
Fig. (8): Variation of ln $\sigma_{ac}(\omega)$, with ln ω for Sb$_2$S$_3$ at different temperatures
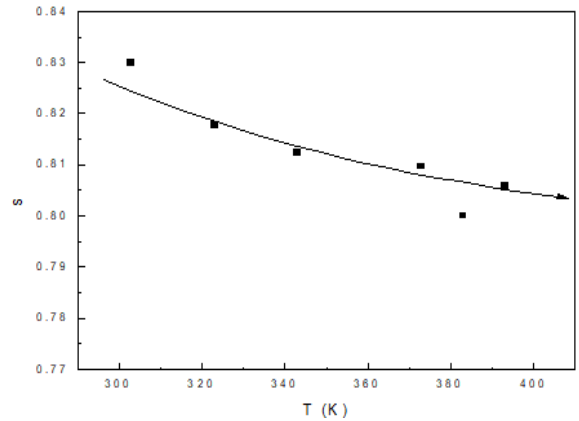
Fig. (9): Temperature dependence of frequency exponent(s) for Sb$_2$S$_3$

Table (1): Results of bulk Sb$_2$S$_3$ compared with other studies

Materials condition	Temperature range (K)	Frequency range (Hz)	Frequency exponent	Mechanism of ac conduction	References
Bulk Sb$_2$S$_3$	303-393	10^2-10^6	0.83-0.79	correlated barrier hopping	The present work
Sb$_2$S$_3$ thin film	303-373	10^2-10^5	1 - 0.7	correlated barrier hopping	[42]
Sb$_2$S$_3$ sprayed thin film	598-698	5-13×10^5	0.79 - 0.49	correlated barrier hopping	[43]

Table (2): Values of density of localized states, N(E$_F$), for Sb$_2$S$_3$ at different temperatures

T (K)	303	323	343	373	383	393
N(E$_F$).10^{18} (eV^{-1}cm^{-3})	8.69	9.23	9.43	10.21	11.21	12.09
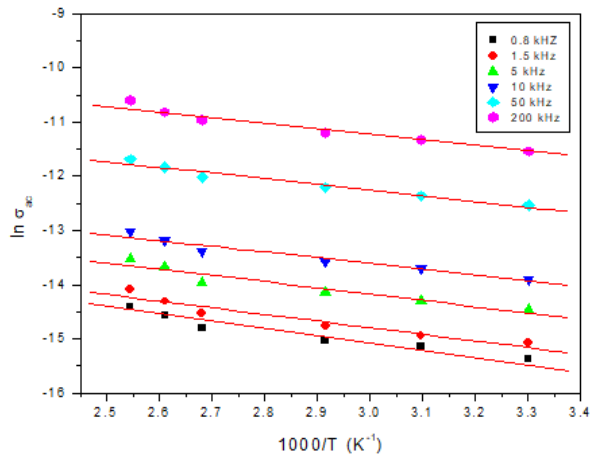
Fig. (10): The variation of ln $\sigma_{ac}(\omega)$ as a function of 1000/T for Sb$_2$S$_3$ at different frequencies
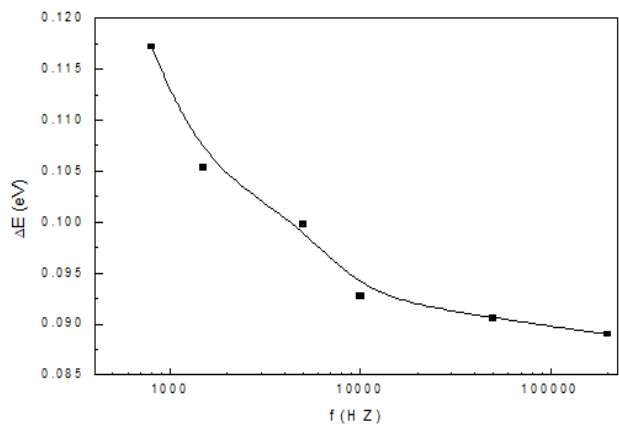
Fig. (11): The variation of ΔE for Sb$_2$S$_3$ against frequency

Conclusion

The structural features of the investigated Sb_2S_3 powder were analyzed by XRD technique. The Sb_2S_3 was found to be consistent with an orthorhombic system with lattice parameters a= 14.20Å, b=11.47 Å and c=7.47 Å. The major diffraction peak corresponds to the preferred orientation of (401). The powder of Sb_2S_3 showed particles of irregular shape which were distributed over the surface in agglomerates. Dielectric properties and ac conductivity of bulk Sb_2S_3 were studied at various temperatures and frequencies. The dielectric constant and dielectric loss decrease with increasing the frequency and increase by increasing the temperature. M' has small values at low frequencies and M'' increases with increasing the frequency which reaches a maximum value and decreases with the further raise in the frequency values. The ac conductivity of bulk Sb_2S_3 increased with the increases in the frequency as $\sigma_{ac}(\omega) = G\omega^s$ and it could be explained according to the correlated barrier hopping model. The ac conductivity displayed a thermally activated process from its relation with temperature. Activation energy for ac conduction was calculated and displayed a decrease by increasing frequency from 117 meV at 800 Hz to 89 meV at 200 kHz. Moreover, as the temperature increases, the density of localized states rises from 8.69×10^{18} to 12.09×10^{18} $eV^{-1}.cm^{-3}$ as the temperature increases at a certain frequency.

References

1. Escorcia-García, J., Becerra, D., Nair, M. T. S. and Nair, P. K., Thin Solid Films 569 (2014) 28.

2. Arun, P. and Vedeshwar, A.G., J. Mater. Sci. 31 (1996) 6507.

3. Ibuke, S. and Yochimatsu, S., J. Phys. Soc. Jpn. 10 (1955) 549.

4. Nair, M.T.S., Pena, Y., Campos, J., Garcia, V.M. and Nair, P.K., J. Electrochem. Soc. 145 (1998) 2113.

5. Rajpure, K.Y. and Bhosale, C.H., Materials Chemistry and Physics 64 (2000) 14.

6. Tsopelas, C., J. Nucl. Med. 42 (2001) 46.

7. Zhang, H., Hu, C., Ding, Y. and Lin, Y., J. Alloy. Compd. 625 (2015) 90.

8. Moon, S., Itzhaik, Y., Yum, J., Zakeeruddin, S.M., Hodes, G. and Grätzel, M., J. Phys. Chem. Lett. 1 (2010) 1524.

9. Malakooti, R., Cademartiri, L., Migliori, A., and Ozin, G. A., J. Mater. Chem. 18 (2008) 66.

10. Petzelt, J. andGriga, J. s, Ferroelectrics 5 (1973) 59.

11. Fujita, T., Kurita, K., Takiyama, K. and Oda, T., J. Phys. Soc. Japan 56 (10) (1987) 3734.

12. Grigas, I.P. and Karpus, A.S., Sov. Phys. Sol. Stat. 9 (1968) 2270

13. Grigas, J., Zadoroznaja, L.A., Liachovitskaja, V.A. and Orliukas, A., Lietuvos Fizikos Rinkinys
(Lithuanian J. Phys.), 16 (1976) 833.

14. Savadogo, O. and Mandal, K.C., Sol. Energy Mater. Sol. Cells 26 (1992) 117.

15. Rajpure, K.Y. and Bhosale, C.H., Mater. Chem. Phys. 64 (2000) 70.

16. Ito, S., Tsujimoto, K., Nguyen, D. C., Manabe, K. and Nishino H., Int. J. Hydrogen Energy 38 (2013) 16749.

17. You, M. S., Lim, C. S., Kwon D. H., Heo, J. H., Im S. H. and Chae, K. J., Org. Electron. physics, Mater. Appl. 21 (2015) 155.

18. Messina, S., Nair, M.T.S. and Nair, P.K., Thin Solid Films 515 (2007) 5777.

19. Perales, E., Lifante, G., Agullo-Rueda, F. and De las Hares, C., J. Phys. D: Appl. Phys .40 (2007) 2440.

20. Krishnan, B., Arato, A., Cardenas E., Das Roy, T.K. and Castillo, G.A., Appl. Surf. Sci. 254 (2008) 3200.

21. Aousgi, F. and Aousgi, M. X., Journal of Optoelectronics and Advanced Materials 12 (2010) 227.

22. Medina-Montes, M.I., Montiel-González, Z., Mathews, N.R. and Mathew, X., Journal of Physics and Chemistry of Solids (2017).

23. Ghosh, C., B.P. Varma, Solid State Communications, 31 (1979) 683.

24. Abdelmoneim, H.M., Indian J. Pure Appl. Phys. 48 (2010) 562.

25. A. Hanumaion, T. Bhimosankaram, S.V. Suryanarayan, g. Kumar, Bull. Mater. Sci. 17 (1997) 405.

26. Arun, P. and edeshwar, A.G. V, J. Mater. Sci. 31 (1996) 6507.

27. Mathew, N. J., Oommen, R., Rajalakshmip, U. and Sanjeeviraja C., Chalcogenide Letters 8(7) (2011) 441.

28. EL-Shazly, A.A., Seyam, M.A.M., EL-Samanoudy, M.M., Ammar, A.H. and Assim, E.M., Appl. Sur. Sci. 198 (2002) 129.

29. Hill, N.E., Vaughan, W.E., Price and M. Davies, A.H., Dielectric Properties and Molecular Behaviour, Van Nostrand Reinhold Company, London (1969).

30. Srivaslava, K. K., Kumar, A., Panwar, O. S. and Lakshminarayan, K. N., J. Non-Cryst. Solids 33 (1979) 205.

31. Barsoum, M., Fundamentals of ceramicsI, New York: McGraw-Hill 543(1977).

32. Stevels, J. M., The electrical properties of glass, in Handbuch der Physik, Vol. edited by S. Flügge ,Springer, Berlin (1957).

33. Farid, A.M., Bekheet, A.E., Vacuum 59 (2000) 932.

34. Mathew, N. J., Oommen, R. and Rajalakshmi, U. P., Chalcogenide Letters 7 (2010) 701.

35. Fouad, S.S., Bekheet, A.E., and Farid, A.M., Physica B 322 (2002)163.

36. Kaiser, M., Physica B 407 (2012) 610.

37. Moynihan, C.T.,Solid State Ionics 105 (1998) 175.

38. Jonscher, A.K., Universal Relaxation Law (Chelsea Dielectrics Press, London, (1996).

39. Chen, R.H., Chang, R.Y. and Shern, S.C., J. Phys. Chem. Solids 63 (2002) 2069.

40. Tiwari, J. P. and Shahi, K., Philosophical Magazine 87 (2007) 4475.

41. Boughalmi, R., Boukhachem, A., Kahlaoui, M., Maghraoui, H. and Amlouk, M., Materials Science in Semiconductor Processing 26 (2014) 593.

42. Jonscher, A. K., Nature 267 (1977) 673.

43. Pollak, M., Philos. Mag. 23 (1971) 519.

44. Pollak, M. and Geballe, T.H., Phys. Rev. B 22 (1961) 1742.

45. Pollak, M. and Pike,, G.E., Phys. Rev. Lett. 28 (1972) 1449.

46. Elliott, Mag. B 36 (1978) 1291.

47. S.R. Elliott, Philos Mag. B 37 (1978) 135.

48. Shimakawa K. Philo.s Mag. 46 (1982)123.

49. I.G. Austin, N.F. Mott, Adv. Phys. 18 (1969) 41.

50. V.K. Bahatnagar, K.L. Bhatiam, J. Non-Cryst. Solids 119 (1990) 214.

51. M.M. El-Nahass, H.A.M. Ali, Solid State Communications 152 (2012) 1084.

52. M.M. El-Nahass, A.A. Attia, G.F. Salem, H.A.M. Ali n, M.I. Ismail, Physica B 434 (2014) 89–94.

53. A.E. Bekheet, Physica B 403 (2008) 4342.